

TRANSFER FUNCTIONS FOR THE ALS LATTICE MAGNETS*

R. Keller, Advanced Light Source Center, E. O. Lawrence Berkeley National Laboratory
University of California, Berkeley, CA 94720 USA

Abstract

The primary purpose of the magnetic measurements performed on the ALS storage-ring lattice-magnets was to ascertain their compliance with the strict tolerances established for this third-generation synchrotron light source. In the course of the data evaluation, a novel approximation method has been developed that leads to four-parameter representations of all magnet transfer-functions, and includes saturation and residual field effects. These transfer functions were used to change the standard working point of the ALS storage ring at 1.5-GeV beam energy from the upper to the lower hysteresis branches, and later to ramp the ring energy from 1.5 GeV to the maximum design value of 1.9 GeV in one uninterrupted process that did not require any intermediate tune correction. Likewise, predicted magnet set values for 1.0-GeV conditions were applied and very closely led to the standard betatron tunes.

1 INTRODUCTION

This paper is concerned with characterizing the integrated fundamental strengths of the ALS [1] lattice magnets in the form of analytical expressions. There are six families of ALS lattice magnets, i.e. bend magnets with substantial gradient producing a defocusing quadrupole component; three families of quadrupoles proper; and two families of sextupoles. During the storage-ring construction-phase, the relative spread of fundamental strengths within each of the six families was the parameter by which the placement of individual magnets along the ring was to be judged; conveniently the spreads turned out to be low enough for all three quadrupole families and the bend magnets to allow arbitrary positioning, but the two sextupole families required insertion of customized current shunts to narrow their spread.

To ascertain the fundamental strengths, and also to obtain reasonable interpolation values between the measured excitation points for energy ramping purposes, the original magnetic measurement data which showed relative errors in the order of 2×10^{-3} had to be smoothed. Furthermore, the ever present drive to push an accelerator's performance beyond the original design limits led to the question how the strengths of the lattice magnets could be extrapolated beyond the highest excitation conditions so far explored, representing an electron beam energy of 1.9 GeV. Analytical approximations are very convenient for both purposes, but the important problem is which type of functions to use for the approximations in order to best represent the magnet properties.

Magnet strengths are commonly expressed using transfer functions,

$$F = T \times I \quad (1)$$

where F is the integrated fundamental strength, $F = \int B_y dz$ for a dipole, $F = \int (B_r/r) dz$ for a quadrupole, etc.; T the transfer function value (assumed to be constant); and I the excitation current. This representation, however, is too simple to take into account seemingly minor effects which are quite relevant for third-generation light-sources with relative strength tolerances of 10^{-3} and below. Therefore a more complicated class of functions was developed in the course of this work to represent magnet strengths under varying excitation conditions. The essential features of these new magnet transfer functions are that they allow to distinguish between the two hysteresis branches; are constant at low excitation values; are free of turning points over their entire range; accurately represent the measured saturation effects; and do not fall off too steeply beyond the highest measured excitation-current value. It is worthwhile noting that simple polynomial approximations do not fulfil most of these conditions. On the other hand, even the best transfer function expressions still require the magnets to be given a well-defined history of excitation that unambiguously defines a working point on either the upper or the lower hysteresis branch.

2 ELEMENTS OF TRANSFER FUNCTIONS

In deriving magnet transfer functions from measured data, one can distinguish three zones of the excitation curve, $F(I)$, dependent on whether 1), residual field effects are dominant, 2), the excitation curve is linear, and 3), saturation effects begin to show, see Fig. 1. In this paper the expression hysteresis is being used rather loosely because none of the magnets has ever been brought to full saturation and the magnetization direction was never reversed for any of them. The maximum excitation currents applied during the magnet measurement activities, however, were nearly equal to the ones that are now being applied in day-to-day conditioning after their installation in the storage ring. Therefore the measured excitation curves can be regarded as truly representative of the actual magnet operation conditions, and we use the term hysteresis loop for the two branches of the excitation curve that are followed when running the current between zero, the power-supply imposed limit, and back again to zero.

*This work was supported by the Director, Office of Energy Research, Office of Basic Energy Sciences, Material Sciences Division, U.S. Department of Energy, under Contract No. DE-AC03-76SF00098.

2.1 Residual field effects

The basic assumption about residual field effects made here is that the two branches of the hysteresis curve are linear and parallel to each other at low currents. A look at the corresponding diagram, Fig. 1, suggests that in this case we can unify the two branches into one curve that starts at the origin if we substitute the actual excitation current I with an effective current $I_{\text{eff}} = I \pm I_c$ where I_c , the coercive current, is subtracted to represent the lower hysteresis branch and added for the upper branch. Equ. (1) then reads:

$$F_{u,l} = T \times (I \pm I_c). \quad (2)$$

where the indices u and l stand for upper and lower branch. In the following formulae, these two indices are left out for the sake of simplicity, and the distinction between the two branches is implied by the \pm sign only.

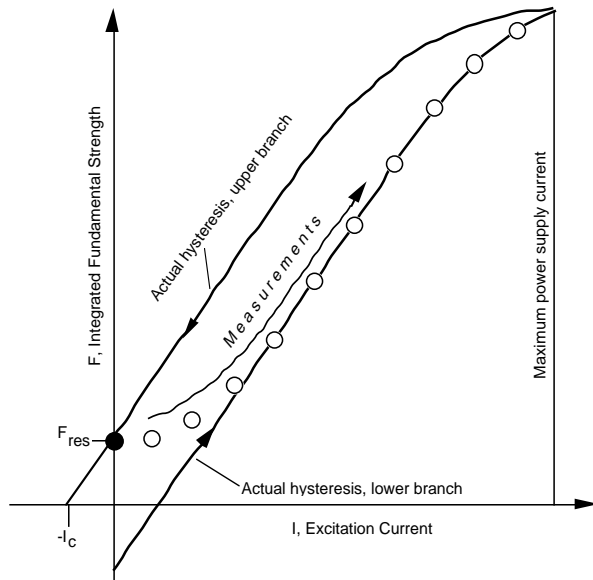


Figure 1. Schematic of a hysteresis loop with magnet measurement data, $F_{i,\text{meas}}$ (open circles). Residual field and saturation effects are exaggerated in this illustration.

In the case of the ALS, the original ten excitation measurements had been taken after completing three unipolar conditioning loops with current settings rising from zero, see Fig. 1; and this fact makes it more complicated to derive a value for the coercive current without direct measurement, even more so because the residual fundamental strength, F_{res} , was not recorded either. The way followed here consists in extrapolating the linear part of the measured excitation curve back to zero strength, thereby determining $-I_c$ and F_{res} , and then reducing all data points $F_{i,\text{meas}}$ in a graded manner:

$$F_{i,\text{red}} = F_{i,\text{meas}} - 2 F_{\text{res}} / \exp \{ I_i / (C I_c) \} \quad [1 \leq i \leq 10] \quad (3)$$

The constant C in the exponential damping term on the right hand side of Equ. (3) is found by empirical optimization, iterating the evaluations of I_c and F_{res} to minimize

the standard deviation for all available, reduced measurement points. The actual values for F_{res} and C are only needed for determination of the constant part of the transfer function, T_{lin} ; once this term is known the sign of I_c is the one parameter that allows to distinguish between upper and lower branch of the hysteresis curve. For the ALS lattice magnets, the optimization was performed empirically on spreadsheets, at first determining individual best values of F_{res} and C for all magnets of one family following a strict standard-deviation optimization and then again, trying to keep the individual values close to the averages for the entire family while allowing the standard deviations to slightly exceed the absolute minimum values.

2.2 Saturation effects

ALS lattice magnets typically show a few percent saturation at excitations corresponding to 1.9-GeV beam energy, and this drop is significant in view of the tolerance band of 10^{-3} relative strength for each magnet type. To represent saturation, Equ. (2) is modified by introducing a denominator,

$$F = \frac{T_{\text{lin}} (I \pm I_c)}{1 + \left(\frac{I \pm I_c}{I_s} \right)^A} \quad (4)$$

and now contains four parameters in addition to the excitation current I as independent variable. The former transfer function T is now called T_{lin} to emphasize that in terms of Equ. (1) it represents the linear part of the excitation curve only.

The evaluation of all five transfer function parameters (including the damping factor C) for every individual magnet is performed in iterations, optimizing residual field and saturation effects in separate loops. After preliminary parameters for each member of one magnet family are established the exponent A and the damping parameter C are averaged for the entire family, and new iterations are performed for each magnet to find the definitive values of the other parameters.

3 ACTUAL TRANSFER FUNCTIONS

An example of a calculated transfer function is given in Fig. 2. In addition to the transfer function calculated according to the formalism developed in the preceding section, the figure displays a “raw transfer function” obtained by simply dividing measured integrated fundamental strengths by the excitation currents, without regard for residual field effects. The low-current part of this curve (broken line) represents the transition from the upper to the lower hysteresis branches.

A list of the averaged calculated transfer function parameters in terms of Equ. (4), as derived from the original measurements [2] for the ALS lattice magnets, is given in Table 1. Note that all entries in the third column are given as integrated flux density values, in units of [T m] divided by the excitation current in [A] and by a nominal radius of

0.03 m elevated to the $(n-1)^{\text{th}}$ power, where $n = 1$ refers to a dipole, $n = 2$ to a quadrupole, and $n = 3$ to a sextupole.

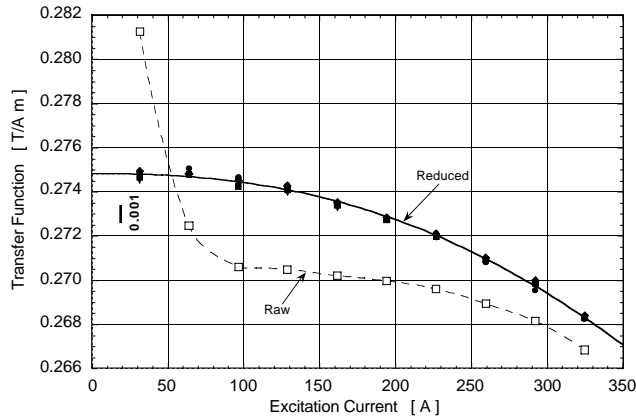


Figure 2. Transfer function for sextupole #10, bold line, evaluated in terms of Equ. (4); the full symbols represent five series of measurements after data reduction. The open symbols represent one of these series before reduction, calculated by dividing the measured fundamental strengths by the corresponding excitation currents according to Equ. (1).

Table 1.

Transfer-Function Parameters for the ALS Lattice Magnets

Type	n	T_{lin} [T A ⁻¹ m ²⁻ⁿ]	I_c [A]	A	I_s [A]
B	1	0.001312	3	5.73	1739
QFA	2	0.01722	2.56	3.1	2250
QF	2	0.05292	0.661	2.8	604
QD	2	0.02875	0.711	4.3	353
SF	3	0.2742	2.767	2.4	1548
SD	3	0.2744	2.844	2.4	1542

4 APPLICATION OF TRANSFER FUNCTIONS

The list of transfer function coefficients of all lattice-magnet families underwent a first critical test when the working points had to be moved from the upper hysteresis branch to the lower one, in view of future energy ramping. Ramping of the storage ring magnets is necessary for all energy levels significantly above 1.5 GeV because this is the design energy-limit of the booster synchrotron that injects beam into the storage ring. The working-point conversion on the base of the predicted set values went smoothly and required only very minor corrections to recover the standard betatron tune values.

To actually ramp the storage ring energy from 1.5 to 1.9 GeV a finely-spaced table of set values (128 steps corresponding to 3 MeV energy increase each) was computed. For every step, Equ. (4) was inverted with a “regula falsi” method to find the proper excitation-current set-values, separately for each magnet family. The variations of the betatron tunes that occurred during the ramping [3] without applying any corrections are displayed in Fig. 3; they correspond to maximum transfer function errors of 8×10^{-4} and

7×10^{-4} for the QF or QD families, respectively, if the total error were ascribed to one of these families only. With the generated ramping tables, the ALS storage-ring energy can now be changed from 1.5 to 1.9 GeV in 64 seconds, without any appreciable loss in beam current.

For operation at 1.0 GeV ramping is unnecessary, and one series of set values has been computed using the entries in Table 1. To fully recover the customary working point at this energy after the calculated magnet current values had been applied, only the QF magnet-family set-currents had to be raised by 0.24%; for all other magnets the calculated values could be used unchanged.

The success in predicting correct set values for all lattice-magnet families under a variety of conditions confirms the validity of the approach developed here. The reader should be warned, however, that the expression for the saturation term in Equ. (4) is valid only as long as the saturation current, I_s , is much larger than the highest applied actual excitation current, I_{max} . This is the case for all magnets discussed in this paper.

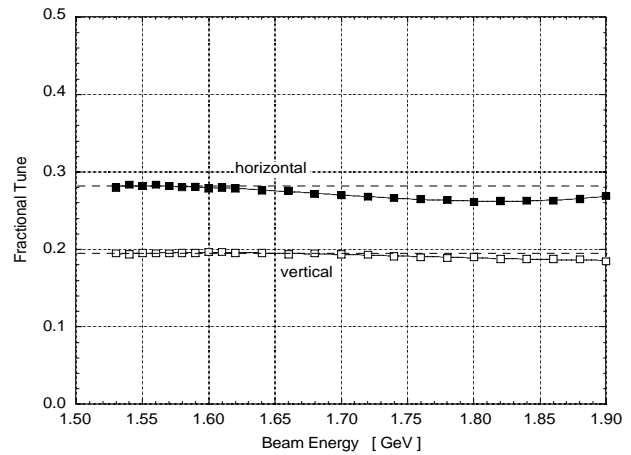


Figure 3. Fractional betatron tunes measured while ramping the storage ring energy with precalculated magnet set values. The full standard tune values at 1.5 GeV are 14.282 (horizontal) and 8.192 (vertical), respectively, as indicated by the straight, broken lines.

5 ACKNOWLEDGMENTS

R. Alvis deserves credit and thanks for diligently processing and plotting the magnet data over and over before the final results as presented here were achieved. Thanks are also due to K. Halbach and A. Jackson for many helpful discussions and to F. Iazzourene, ELETTRA Trieste, for reviewing the employed algorithms and pointing out an inconsistency.

6 REFERENCES

- [1] "1-2 GeV Synchrotron Radiation Source, Conceptual Design Report," LBL Pub. 5172 Rev., LBL Berkeley, 1986.
- [2] Measurements performed at LBL Berkeley under the guidance of J. Tanabe, D. Nelson, and M. I. Green, 1991.
- [3] The code for the control-system application that executed the ramping table was written by H. Nishimura, LBNL Berkeley, unpublished work (1995).